Two-Dimensional Lipid Mixing Entropy Regulates the Formation of Multicomponent Lipoplexes

Giulio Caracciolo,* Daniela Pozzi, and Ruggero Caminiti

Dipartimento di Chimica, Università degli Studi di Roma "La Sapienza", P.le A. Moro 5, 00185 Rome, Italy

Heinz Amenitsch

Institute of Biophysics and Nanosystems Research, Austrian Academy of Sciences, Schmiedelstrasse 6, A-8042 Graz, Austria

Received: April 4, 2006; In Final Form: August 20, 2006

The mechanism of formation of multicomponent lipoplexes was investigated by means of synchrotron Small-Angle X-ray Diffraction (SAXD). Mixed lipid dispersions were prepared by mixing different populations of binary cationic liposomes. When adding DNA to mixed lipid dispersions, multicomponent lipoplexes spontaneously formed exhibiting structural properties, i.e., membrane thickness, surface charge density, and one-dimensional DNA packing density, intermediate between those of binary lipoplexes. These results suggested that DNA lets liposomes come into contact and fuse and that a complete lipid mixing at the molecular level occurs. The equilibrium structure of multicomponent lipoplexes was found to be unique and did not depend on the number and kind of populations composing lipid dispersion but only on the lipid species involved and on their relative molar ratio. According to recent theoretical models we identified two-dimensional lipid mixing entropy as the key factor regulating the existence of only multicomponent lipoplexes with ideally mixed lipid species.

I. Introduction

When adding DNA to an aqueous solution of liposomes composed of cationic and neutral lipids, cationic lipid−DNA complexes (lipoplexes) spontaneously form. Synchrotron X-ray diffraction experiments made it possible to resolve the internal microscopic structure of lipoplexes and to quantify the DNA packing density within.[1−6] Lipoplexes have a highly ordered structure whose topology is controlled by the neutral "helper" lipid. Helper lipids favoring planar bilayers force lipoplexes to be assembled in a multilayer structure with alternating lipid bilayers and DNA monolayers (L_α^C phase, Figure 1). Neutral lipids with a membrane negative spontaneous curvature promote the formation of lipoplexes assembled in a two-dimensional (2D) inverted hexagonal phase with water gaps filled by DNA strands (H_{II}^C phase, Figure 1).

Lipoplexes are currently the most promising nonviral gene delivery vectors even though their transfection efficiency is lower than that of viruses. First it was hypothesized that a strict connection between lipoplex structure and transfection efficiency existed leading to the misconception that H_{II}^C lipoplexes transfected more efficiently than L_α^C ones.[2] When experimental evidence was provided that lamellar complexes can compete in transfection with hexagonal ones,[7,8] it appeared clear that many other aspects of lipoplex-mediated transfection had to be investigated. Nowadays it is believed that improving transfection will require decoding all the molecular mechanisms ranging from lipoplex formation to interactions between complexes and cellular components.[9−13]

In this paper, we addressed the mechanism of formation of lipoplexes by means of synchrotron small-angle X-ray diffraction (SAXD). To this end, we first characterized the equilibrium structures of several binary lipoplexes made of binary CLs and linear DNA. Then we looked at the simultaneous interaction of distinct populations of binary CLs with DNA. Comparing emerging nanostructures with those of binary lipoplexes we could shed light on the mechanism of formation of lipoplexes. Here we show that, when adding DNA to lipid dispersions containing different populations of liposomes, well-ordered multicomponent L_α^C nanostructures emerge and that no binary lipoplexes exist. It means that DNA induces aggregation and fusion of distinct liposomes and that, upon DNA-induced fusion of liposomes, an almost ideal lipid mixing at the molecular level

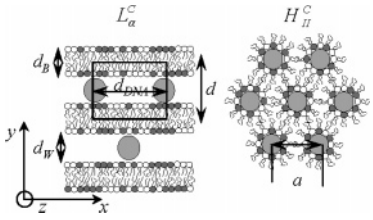

Figure 1. Schematics of the inner structure of lamellar L_α^C and hexagonal H_{II}^C CL-DNA nanostructures. In the lamellar phase (left) DNA rods are intercalated between cationic lipid membranes in the liquid-crystalline phase composed of cationic (grey) and neutral helper (white) lipids. The lamellar spacing, d, is the sum of the lipid bilayer thickness, d_B, plus the thickness of the interbilayer water layer, d_W. The DNA spacing, indicated as d_{DNA}, is the distance between adjacent DNA rods. The two-dimensional inverted hexagonal phase, H_{II}^C (right), is made up of infinitely long rigid rods, all identical and crystallographically equivalent, regularly packed in a 2D hexagonal lattice. The cylinders are filled by water and are dispersed in the continuous medium constituted by hydrocarbon chains, whereas the polar groups are located at the water−hydrocarbon chain interface. Water gapes are filled by DNA strands.

* Address correspondence to this author. Phone: +39 06 4991 3076. Fax: +39 06 490631. E-mail: g.caracciolo@caspur.it.

10.1021/jp0620926 CCC: $33.50
Published on Web 10/05/2006

occurs. By using a functional of free energy calculated for L_α^C lipoplexes by Harries et al.,[14] here we demonstrate that spontaneous formation of multicomponent lipoplexes is a thermodynamic process driven by two-dimensional (2D) lipid mixing entropy.

Furthermore, physical properties of lipoplexes such as lipid bilayer thickness, thickness of interbilayer water gaps, surface charge density of lipid bilayers, and DNA packing density were modified simply by adjusting the composition of mixed lipid dispersions. It was a significant result. Indeed, the engineering of multicomponent lipoplexes, incorporating the specific properties of very different lipid species, may represent the starting point for rationally designing highly specific gene vectors.[15,16]

II. Experimental Methods

A. Liposomes Preparation. 1,2-Dioleoyl-3-trimethylammonium-propane (DOTAP), dioleoylphosphatidylethanolamine (DOPE), (3-[*N*-(*N*′,*N*′-dimethylaminoethane)carbamoyl]cholesterol (DC-Chol), and dioleoylphosphocholine (DOPC) were purchased from Avanti Polar Lipids (Alabaster, AL) and used without further purification. Multilamellar DOTAP/DOPE (A), DOTAP/DOPC, (B), DC-Chol/DOPE (C), and DC-Chol/DOPC (D) binary cationic liposomes (CLs) were routinely prepared.[17] Briefly, each binary mixture, at a molar ratio of neutral lipid in the bilayer Φ = (neutral lipid/total lipid) (mol/mol) = 0.5, was dissolved in chloroform and the solvent was evaporated under a vacuum for at least 12 h. The lipid films obtained were hydrated with the appropriate amount of Tris-HCl buffer solution (10^{-2} M, pH 7.4) to achieve the desired final concentration. The solutions were incubated at 30 °C for 6 h to allow formation of CLs. The same procedure was followed to prepare DOTAP/DOPE/DC-Chol/DOPC (E) quaternary CLs. A-D mixed lipid dispersions were prepared by mixing A and D vesicles at molar ratio $R = A/(A + D) = 0.5$. In the same way, B-C and A-B-C-D mixed lipid dispersions were prepared and allowed to balance at 30 °C for 24 h.

B. Lipoplexes Preparation. Calf thymus Na-DNA was purchased from Sigma (St. Louis, MO). DNA was dissolved in Tris-HCl buffer (10 mg/mL) and was sonicated for 5 min inducing a DNA fragmentation with length distribution between 500 and 1000 base pairs, which was determined by gel electrophoresis. Lipoplexes made of binary CLs and DNA will be referred to as "binary lipoplexes" to indicate that lipid bilayer is a binary mixture of cationic and neutral lipids. By mixing adequate amounts of the DNA solution to suitable volumes of A, B, C, and D dispersions, self-assembled DOTAP/DOPE-DNA (A-DNA), DOTAP/DOPC-DNA, (B-DNA), DC-Chol/DOPE-DNA (C-DNA), and DC-Chol/DOPC-DNA (D-DNA) binary lipoplexes were obtained.

In what follows we shall denote indifferently as "quaternary lipoplexes" or multicomponent lipoplexes the complexes whose lipid membrane contains four lipid species simultaneously. Multicomponent lipoplexes were prepared following four different preparation schedules. In the first case DNA was added to a mixed dispersion of A and D liposomes. In the second case DNA was added to a mixed dispersion of B and C liposomes. In the third case, DNA molecules were added to a mixed dispersion containing A, B, C, and D liposomes. Last, DNA was added to E quaternary liposomes to prepare E-DNA quaternary lipoplexes. By adding appropriate amounts of DNA solution to lipid dispersions lipoplexes at the charge ratios ρ = (lipid charge/DNA charge) = 1 and 2 were prepared.

C. SAXD Experiments. All SAXD measurements were performed at the Austrian SAXS station of the synchrotron light source ELETTRA (Trieste, Italy).[18] SAXD patterns were recorded with a gas detector based on the delay line principle covering a q-range ($q = 4\pi \sin(\theta)/\lambda$) of between 0.05 and 1.5 Å^{-1}. The angular calibration of the detector was performed with silver-behenate [$CH_3(CH_2)_{20}$-COOAg] whose d corresponds to 58.38 Å. The unoriented samples were sealed in 1.5 mm diameter glass X-ray capillaries. Exposure times were between 100 and 500 s. No evidence of radiation damage was observed in any sample at these exposure times. The Tris-HCl bulk solution was subtracted as background from the collected data. All SAXD measurements were performed at 26 °C and temperature was controlled close to the capillary by a KPR-Peltier module (Anton Paar, Graz, Austria) with a precision of 0.1 °C.

D. Data Analysis. Due to the bilayer nature of lipid membranes, the electron density profile (EDP) is centrosymmetric therefore the electron density profile, $\Delta\rho$, along the normal to the bilayer, z, can be calculated as a Fourier sum of cosine terms,

$$\Delta\rho = \frac{\rho(z) - \langle\rho\rangle}{[\langle\rho^2(z)\rangle - \langle\rho\rangle^2]^{1/2}} = \sum_{l=1}^{N} F_l \cos\left(2\pi l \frac{z}{d}\right) \qquad (1)$$

where $\rho(z)$ is the electron density, $\langle\rho\rangle$ is its average value, N is the highest order of the fundamental reflection observed in the XRD pattern, F_l is the form factor for the (00l) reflection, and d is the lamellar periodicity along the normal to the lipid bilayer consisting of one lipid bilayer and one water layer. Form factors F_l were calculated from the integrated intensity $I_l = F_l^2/C_l$ under the lth diffraction peak, where $C_l = q_l^2$ is the Lorentz-polarization correction factor for unoriented samples and the diffraction geometry used. The phase choice for each lipid mixture, i.e., the correct sign combination used to calculate the electron density profile, was found in order that the profiles exhibited the usual lipid bilayer density plus an additional maximum in the middle of the water region due to the DNA chains.[19]

III. Results

Figure 2 shows the SAXD patterns of binary A-DNA (panel a), B-DNA, (panel b), C-DNA (panel c), and D-DNA (panel d) charge-neutral lipoplexes ($\rho = 1$). In panel a, two distinctly labeled sets of peaks are identified, which can be indexed on a multilamellar L_α^C phase and on 2D H_{II}^C nanostructure.

Lamellar peaks at q_{00n} arose from the multilamellar L_α^C phase ($d = 2\pi/q_{001} = 65.2$ Å) consisting of smectic-like arrays of stacked bilayers with monolayers of DNA molecules intercalated within the water gaps (Figure 1). The DNA peak (marked by an arrow) occurring at $q_{DNA} = 0.183$ Å^{-1} ($d_{DNA} = 2\pi/q_{DNA} = 34.3$ Å) arose from diffraction from the one-dimensional lattice of DNA chains embedded between lipid bilayers (Figure 1). The second set of Bragg peaks, positioned at $q_{10} = 0.109$ Å^{-1}, $q_{20} = 0.218$ Å^{-1}, and $q_{21} = 0.287$ Å^{-1}, arose from a two-dimensional H_{II}^C phase with a unit cell spacing of $a = 4\pi/[(3)^{0.5}q_{10}] = 66.6$ Å. The structure of the H_{II}^C phase resembles that of the H_{II} phase of pure DOPE in excess water, with the water space inside the lipid micelle filled by DNA. Our findings are in excellent agreement with those previously reported by Koltover et al.,[5] who found coexistence, for DOTAP-DOPE mixed membranes, of L_α^C and H_{II}^C phases. The scattering distributions of B-DNA, C-DNA, and D-DNA lipoplexes (panels b, c, and d, respectively) indicated a well-ordered lamellar structure of stacked membranes with different

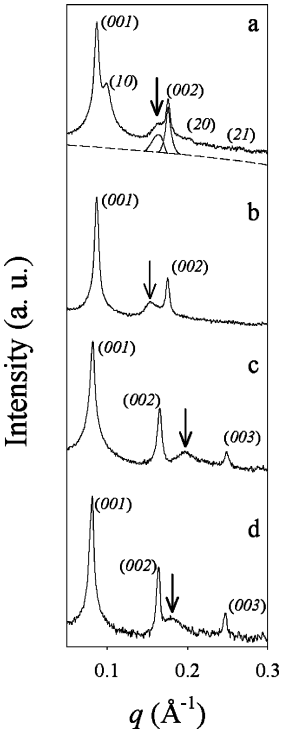

Figure 2. Synchrotron SAXD patterns of binary DOTAP/DOPE-DNA (A-DNA, panel a), DOTAP/DOPC-DNA (B-DNA, panel b), DC-Chol/DOPE-DNA (C-DNA, panel c), and DC-Chol/DOPC (D-DNA, panel d) lipoplexes ($\rho = 1$). Bragg peaks labeled as (00l) arise from the L_α^C phase whereas (0l) ones (panel a) arise from the H_{II}^C phase. The DNA peak of the lamellar phases is marked by an arrow. For clarity, the q-range is restricted to between 0.05 and 0.3 Å^{-1}.

TABLE 1: Structural Parameters of A-DNA (DOTAP/DOPE-DNA), B-DNA (DOTAP/DOPC-DNA), C-DNA (DC-Chol/DOPE-DNA), and D-DNA (DC-Chol/DOPC-DNA) Lipoplexes ($\rho = 1$) Calculated from the EDPs of Figure 3[a]

	d (Å)	d_B (Å)	d_W (Å)	d^{exp}_{DNA} (Å)	d^{th}_{DNA} (Å)	σ_M (10^{-3} e/Å^2)
A-DNA	65.2	37.8	27.4	34.3	37.5	8.2
B-DNA	65.3	39.2	26.1	37.4	37.3	7.4
C-DNA	69.2	41.5	27.7	29.2	30.3	8.5
D-DNA	69.7	41.8	27.9	31.8	31.4	7.6

[a] Theoretical DNA-DNA spacings, d^{th}_{DNA}, were calculated from eq 2.

periodicities, d, as listed in Table 1. From the full width at half-maximum (fwhm) of the first-order lamellar Bragg peaks, a domain lamellar size of about $L_m = 2\pi/\text{fwhm} \approx 5000$ Å could be estimated. It is a lower limit of L_m because the experimental fwhm may be larger than the true value because of the peak spreading due to the convolution with the intrinsic instrumental resolution function. In the isoelectric regimes, charge-neutral lipoplexes usually exhibited a globular structure (data not reported) with globule diameters of about 1 μm. Since an upper bound for L_m is given by the diameters of the globules, we can conclude that binary lipoplexes consist of just one, or two, lamellar domains.

With the aim of providing all the relevant structural parameters, electron density profiles along the normal to lipid bilayers were calculated from the SAXD patterns of Figure 2 and are shown in Figure 3. X-ray data from multilamellar arrays can yield electron density profiles only along the normal to the bilayers, giving a measure of the bilayer thickness, d_B, and the size of the water region, d_W (Figure 1). The electron-denser regions, i.e., the two maxima in the electron density profiles of

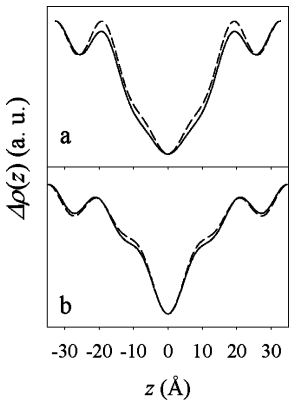

Figure 3. Electron density profiles of DOTAP/DOPE-DNA (continuous line) and DOTAP/DOPC-DNA (dotted line) (top panel). The bottom panel is a comparison between electron density profiles of DC-Chol/DOPE-DNA (continuous line) and DC-Chol/DOPC (dotted line).

Figure 3, represent the headgroups region, while the pronounced central minimum, at $z = 0$, corresponds to the terminal methyl groups of the opposing acyl chains. The distance between the maxima provides a reasonable estimate of the membrane thickness, d_B. According to general definitions,[20] the lamellar repeat distance d can be regarded as the sum of the membrane thickness, d_B, and the water layer thickness, d_W (Figure 1). Thus, the interbilayer water thickness is usually defined as $d_W = d - d_B$.

In Figure 3, panel a, comparison between the profiles of DOTAP/DOPE-DNA (continuous line) and DOTAP/DOPC-DNA (dotted line) is shown. We observed that the spatial extension of the lipid headgroup region, d_H, estimated from the fwhm of the Gaussian maxima of the EDPs,[21] is roughly the same ($d_H \approx 8$ Å). This finding seems quite reasonable since, for phosphatidylcholines, d_H is usually set to 9 Å. The slightly denser DOPC headgroup just results in a more pronounced maximum of electron density. In Figure 3, panel b, EDPs of DC-Chol/DOPE-DNA (continuous line) and DC-Chol/DOPC-DNA (dotted line) are compared. As can be seen, the Gaussian maxima are definitely less pronounced than those of EDPs of DOTAP-containing membranes. A molecular interpretation can be given if the difference in the chemical structure of the cationic lipids is considered. Indeed, the headgroup of DOTAP exhibits higher electron density than that of DC-Chol and does produce stronger maxima in the EDPs.

From the EDPs of Figure 3 we calculated the values of d_B and d_W of binary lipoplexes which are reported in Table 1. Apart from the lamellar peaks, all the SAXD patterns of Figure 2 also exhibited a much broader peak arising from the DNA-DNA in-plane correlation (marked by an arrow). The DNA in-plane lattice is well described by the following relationship, which results from simple mass conservation in multilamellar geometry[3]

$$d_{DNA} = \frac{A_D \rho_D}{d_B \rho_L}(L/D) \qquad (2)$$

where $A_D = 190$ Å^2 is the cross-section area of the DNA molecule, $\rho_D = 1.7$ g/cm^3 and $\rho_L = 1.07$ g/cm^3 are densities of DNA and lipid, and (L/D) is the total lipid/DNA weight ratio.

Except for A-DNA lipoplexes, the calculated values show very good agreement with the experimental values (Table 1). As recognized, the surface charge density, σ_M, is the only physical constraint regulating the DNA in-plane rod lattice. Thus, one would expect very similar DNA-DNA spacings for

A-DNA and B-DNA lipoplexes. Conversely, considering the case of A-DNA lipoplexes, we observed a d_{DNA} value much shorter than that theoretically expected (34.3 Å with respect to 37.5 Å). To address this issue, one has to bear in mind that A-DNA lipoplexes exhibit coexistence of L_α^C and H_{II}^C phases (Figure 2, panel a). In principle, lipid molecules could not be ideally mixed, the two coexisting phases having different lipid composition. As recently proposed,[16] this means that the hexagonal H_{II}^C phase could be richer in DOPE than in DOTAP because the former, due to its natural negative curvature, self-assembles in 2D hexagonal phases. Accordingly, the effective molar fraction of DOTAP in the lamellar L_α^C phase would be higher than that expected thus resulting in a DNA packing density higher than one would expect in all lamellar complexes at the same charge ratio ρ. An estimate of the surface charge density of lipid membranes can be provided by the following relationship[15,29]

$$\sigma_M = \frac{(1-\Phi_W)}{(1-\Phi_M)}\frac{1}{2ld_{DNA}} \quad (3)$$

where Φ_W and Φ_M are the weight and molar ratios of neutral to total lipid in the bilayer and l is the distance between two phosphates projected onto the DNA axis ($l = 1.7$ Å). Therefore, the observed enlargement of the DNA in-plane rod lattice may be interpreted in terms of reduction of surface charge density (Table 1).

Having characterized the structure of binary lipoplexes in detail, we then investigated the structure of quaternary lipoplexes. SAXD measurements carried out on mixed dispersions containing DOTAP/DOPE and DC-Chol/DOPC liposomes with no DNA added revealed (data not reported) that no fusion between liposomes had occurred. No fusion between liposomes was observed even when DOTAP/DOPC and DC-Chol/DOPE liposomes were mixed. It means that electrostatic charges localized on the surface of liposomes create a repulsive barrier that strongly dominates over short-range attractive van der Waals forces and prevents membrane aggregation and fusion.[15,16,22−25]

Adding DNA to both the mixed dispersions produced major changes in the lipid structure.

First, DNA was added to a mixed dispersion containing A and D liposomes whereas, second, DNA was added to a dispersion containing B and C liposomes.

Figure 4 shows the SAXD patterns of quaternary A-D-DNA (panel a) and B-C-DNA lipoplexes (panel b). The SAXD patterns of Figure 4 show that, upon mixing DNA to mixed lipid dispersions, only one kind of mixed lipoplex exists. In principle, one could expect binary lipoplexes to coexist within the sample volume. Conversely, when adding DNA to dispersions containing coexisting A and D CLs or, alternatively, B and C CLs, A-D-DNA and B-C-DNA mixed lipoplexes spontaneously form. Our strongest experimental argument for the existence of only mixed complexes is, first, that the SAXD patterns of Figure 4 do not arise from superposition of the SAXD patterns of Figure 2 and, second, that the fwhm of all the Bragg reflections of "quaternary lipoplexes" is roughly the same as in "binary lipoplexes". Support for this interpretation was provided by DNA packing density within mixed lipoplexes. It is well-known that lamellar lipoplexes can adjust the interaxial spacing, d_{DNA}, to minimize the total free energy by separating the DNA strands.[5,26−29] Thus, if lipid mixing was not almost ideal and different local surface charge densities existed, they would produce locally dissimilar DNA packing densities, in turn

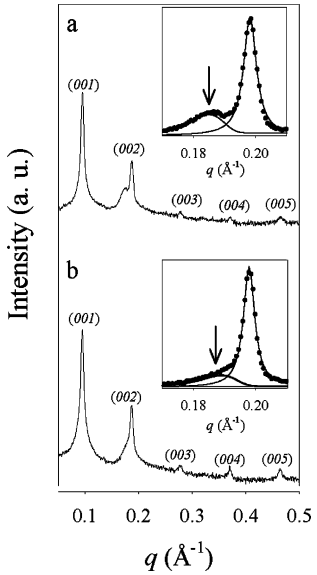

Figure 4. SAXD patterns of quaternary A-D-DNA (panel a) and B-C-DNA lipoplexes (panel b). The inset shows a view of the second-order Bragg peak region on an expanded vertical scale. Full lines show the fitting functions.

TABLE 2: Structural Parameters of A-D-DNA (DOTAP/DOPE-DC-Chol/DOPC-DNA) and B-C-DNA (DOTAP/DOPC-DC-Chol/DOPE-DNA) Lipoplexes ($\rho = 1$) Calculated from the EDPs

	d (Å)	d_B (Å)	d_W (Å)	d^{exp}_{DNA} (Å)	d^{th}_{DNA} (Å)	σ_M (10^{-3} e/Å^2)
A-D-DNA	65.9	38.2	27.7	33.7	33.7	7.8
B-C-DNA	66.2	38.4	27.8	33.1	33.5	8.0

resulting in distinct DNA peaks in the SAXD pattern. In contrast, we noted that the SAXD patterns of Figure 4 exhibit a single DNA peak (marked by an arrow).

All these observations allowed us to conclude that, upon liposome fusion, there is a large onset of membrane mixing. Ideally mixed multicomponent lipoplexes can exist only if binary liposomes break up during lipoplex formation and a complete lipid mixing at the molecular level occurs.

As liposome fusion could not be observed merely by mixing binary CLs, it was therefore the DNA that allowed the repulsive barrier to be overcome and the liposomes to come into contact, aggregate, and fuse. DNA acted therefore as a molecular glue enforcing close apposition of vesicles, contact, and fusion.[30] The lipid bilayer, being a fluid mixture, allows for lateral diffusion of lipid molecules leading to a spatial distribution of the four lipid species, on average, uniform.[31,32] Having recognized that only mixed lipoplexes exist, we investigated the structural properties of emerging lipoplexes in detail. EDPs, calculated from the SAXD patterns of Figure 4, allowed us to conclude that A-D and B-C lipid bilayers exhibit identical physical properties, such as bilayer thickness, thickness of the water gaps, and surface charge density (Table 2). Furthermore, we also underline that physical properties of multicomponent lipoplexes are intermediate between those of binary lipoplexes. This finding is of central importance since it opens the door to the rational designing of multicomponent lipoplexes to be performed just by varying the composition of lipid dispersions.

To investigate the interplay between the composition of mixed lipid dispersion and the lipid species involved more deeply, we subsequently prepared quaternary lipoplexes by adding DNA to a dispersion containing coexisting A, B, C, and D binary CLs being careful to maintain the equimolar ratio between all

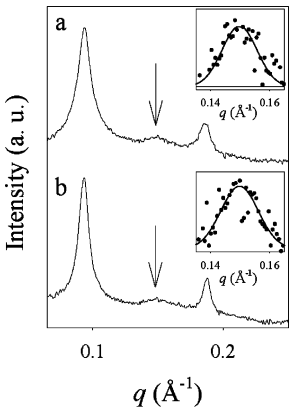

Figure 5. Comparison between the SAXD pattern of quaternary A-B-C-D-DNA lipoplexes (panel a) and E-lipoplexes (panel b). Both patterns show an identical set of equally spaced (00*l*) Bragg reflections corresponding to the lamellar stacking of the lipid membrane plus the water gap occupied by DNA molecules. The inset shows a view of the DNA Bragg peak. For clarity, the *q*-range is restricted to between 0.05 and 0.25 $Å^{-1}$.

TABLE 3: Structural Parameters of A-B-C-D-DNA (DOTAP/DOPE-DOTAP/DOPC-DC-Chol/DOPE-DC-Chol/DOPC-DNA) and E-DNA (DOTAP/DOPE/DC-Chol/DOPC-DNA) Lipoplexes ($\rho = 2$) Calculated from the EDPs

	d (Å)	d_B (Å)	d_W (Å)	d^{exp}_{DNA} (Å)	σ_M (10^{-3} e/Å^2)
A-B-C-D-DNA	66	38.2	27.8	41.9	8.0
E-DNA	66.2	38.4	27.8	41.9	8.0

lipid species at the lipid/DNA molar ratio $\rho = 1$. Again the equilibrium structure of lipoplexes was found to be the same (not reported).

Nevertheless, differences in the physical properties of lipoplexes could depend on whether liposomes interact with a small or a large amount of DNA.[30] Thus, to extend our conclusions to the biologically relevant positively overcharged lipoplexes, we added DNA at the lipid/DNA molar ratio $\rho = 2$.

Figure 5 shows the comparison between the SAXD pattern of quaternary A-B-C-D-DNA lipoplexes (panel a) and E-lipoplexes (panel b). Both patterns show an identical set of equally spaced (00*l*) Bragg reflections corresponding to the lamellar stacking of the lipid membrane plus the water gap occupied by DNA molecules. While the position of the reflections is, within experimental error, the same, their fwhm is slightly different varying from 0.0024 (E-DNA) to 0.0030 $Å^{-1}$ (A-B-C-D-DNA). Thus E-DNA lipoplexes show a slightly higher long-range order than that of A-B-C-D-DNA lipoplexes.

Bearing in mind that E-DNA lipoplexes were prepared by adding DNA directly to quaternary liposomes, our latter findings confirm unambiguously that, upon DNA-induced liposome fusion, complete lipid mixing occurs. Accordingly, structure and membrane physical properties of A-B-C-D-DNA and E-DNA lipoplexes were found to be equal (Table 3). Even more remarkably, it was really striking to observe that the structural properties of both A-B-C-D-DNA and E-DNA lipoplexes were also equal to those of A-D-DNA and B-C-DNA quaternary lipoplexes. The DNA lattice, $d_{DNA} \approx 42$ Å, was larger than that observed in the case of A-D-DNA and B-C-DNA lipoplexes due to a higher ρ ratio. Anyway, differences in domain lamellar size could be noted. From the width of the (001) lamellar Bragg peak, a value of $L_m \approx 2000$ Å could be calculated. Positively charged complexes aggregated into clusters with diameters of 0.4 μm. As observed in the isoelectric regime, our results show that aggregates consist of two lamellar domains.

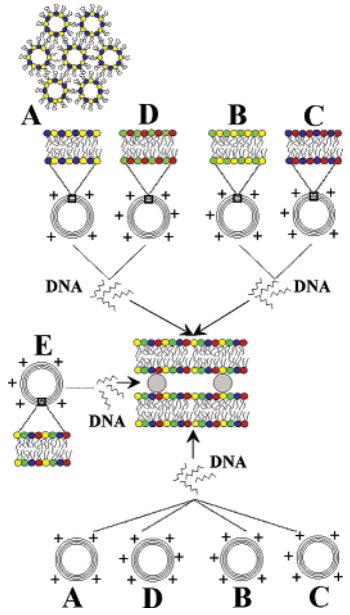

Figure 6. Mechanism of formation of mixed multicomponent lipoplexes. When adding DNA to one mixed dispersion containing DOTAP/DOPE (A) and DC-Chol/DOPC (D) binary cationic liposomes (top, on the left) or to a dispersion containing DOTAP/DOPC (B) and DC-Chol/DOPE (C) binary cationic liposomes (top, on the right), multicomponent mixed lipoplexes spontaneously form. DNA induces aggregation and fusion of liposomes and a large lipid mixing occurs. As a result, only multicomponent A-B-C-D-DNA lipoplexes exist (3). Identical lipoplexes can be formed by adding DNA to a mixed dispersion containing A, B, C, and D binary liposomes at once or, alternatively, to one dispersion of quaternary DOTAP/DOPE/DC-Chol/DOPC CLs. The formation of multicomponent lipoplex does not depend therefore on which liposomes the lipid dispersion is composed of, the only relevant condition being the equimolar composition of lipid species. Thus, multicomponent lipoplex formation is a spontaneous process driven by thermodynamics.

In conclusion, the general meaning of our experimental findings is that the formation of multicomponent lipoplex does not depend on which liposomes the lipid dispersion is composed of, the only relevant condition being the equimolar composition of lipid species. Accordingly, several pathways can be followed as schematically summarized in Figure 6. All these observations suggest that multicomponent lipoplex formation is a spontaneous process thus driven by thermodynamics.

IV. Discussion

Several energy barriers opposing the mixing process exist. Indeed positive electrostatic charges localized on the surface of liposomes create a repulsive barrier that prevails over short-range attractive van der Waals forces and avoids membrane aggregation and fusion. Furthermore, lipid molecules are held in bilayers by hydrophobic interactions and a change in supramolecular organization—such as required by the mixing process—is definitely opposed by this strong energy barrier. Conversely, when DNA is added, the mixing process takes place spontaneously. This means that DNA allows liposomes to come into contact, break, and fuse by reducing the energy barrier due to electrostatic, hydrophobic, steric, and hydration interactions. Aside from giving a quantitative description of the early stages of interaction, we address molecular mechanisms occurring when diffusion of lipid molecules is freely permitted and energetic barriers have already been overcome by DNA.

Since the lipid bilayer is a 2D fluid mixture, the lipid molecules are free to diffuse within the membrane plane. To

explain the spontaneous formation of multicomponent lipoplexes we first need the formation free energies of the complexes. According to Harries et al.,[14] a general free energy functional including all relevant contributions to the binary lipoplex free energy is given by

$$F = \int_V \frac{\epsilon}{2}(\nabla\Phi)^2\,\mathrm{d}V + k_\mathrm{B}T\int_V\left[n_+\ln\frac{n_+}{n_0} + n_-\ln\frac{n_-}{n_0} - (n_+ + n_- + 2n_0)\right]\mathrm{d}V + \frac{k_\mathrm{B}T}{a}\int_S[\eta\ln\eta + (1-\eta)\times \ln(1-\eta)]\,\mathrm{d}S + \chi\frac{k_\mathrm{B}T}{a}\int_S[\eta(1-\eta)]\,\mathrm{d}S + \chi\frac{3k_\mathrm{B}T}{a}\int_S(\nabla\eta)^2\,\mathrm{d}S \quad (4)$$

The first term here is the electrostatic free energy, where ϵ is dielectric constant of water, and Φ is the electrostatic potential. The integration extends over the whole volume of the solution. The second term is due to the entropy of mobile counterions in solution with n_+, n_- representing the local densities of positively and negatively charged ions and n_0 their bulk density. The third term represents the 2D lipid mixing entropy, F^{MIX}, with $\eta = \eta(x,z)$ being the local density of charged lipid molecules in the plane of the membrane and a the interfacial area per lipid molecule. The fourth and fifth terms only survive when the lipid mixture is not ideal with a degree of nonideality χ.

In the case of binary lipoplexes, the 2D lipid mixing entropy of eq 4 reads

$$F^{\mathrm{MIX}} = \frac{k_\mathrm{B}T}{a}\int_S[\eta\ln\eta + (1-\eta)\ln(1-\eta)]\,\mathrm{d}S \quad (5)$$

where S is the area of the membrane over which integration extends.

Experimentally we found that only mixed multicomponent complexes existed and no binary lipoplexes were present within the sample volume. By using eq 5 we shall demonstrate that, when adding DNA to mixed lipid dispersions (such as the case of A-D or B-C liposomes), the formation of quaternary lipoplexes ideally mixed is thermodynamically favored with respect to the formation of separated binary lipoplexes.

The L_α^C is an ordered smectic-like array with a periodic structure in the plane (x,y) perpendicular to the DNA axis that we label as the z-axis.[28,29] The complex is invariant upon translation along the z axis (Figure 1) so that a unit cell is usually specified by the distance between opposing lipid surfaces, d_W, the thickness of the lipid bilayer, d_B, and the DNA-DNA repeat distance, d_{DNA}. The complex is regarded as a one-dimensional lattice of DNA molecules modeled as infinite rods sandwiched between alternating lipid bilayers. Let us consider two adjacent unit cells of the complex. For clarity, the case of separated binary lipoplexes coexisting within the sample volume will be modeled by considering two adjacent unit cells each consisting of a binary lipid mixture with intercalated DNA strands (Figure 7, top panel). On the other hand, quaternary mixed lipoplexes will be taken into account by an analogous arrangement with four lipid species ideally mixed (Figure 7, bottom panel). As a result of such a molecular arrangement, two different profiles of local density of one charged lipid in the plane of the membrane (indifferently DOTAP or DC-Chol) arose. We labeled them as $\eta_1 = \eta_1(x,z)$ and $\eta_2 = \eta_2(x,z)$.

When unmixed binary lipoplexes coexist within the sample volume (Figure 7, top panel), the average fraction of one charged lipid is therefore $\langle\eta_1\rangle = 0.5$ in the first unit cell and decays to $\langle\eta_1\rangle = 0$ in the second one. Conversely, the average fraction of the other charged lipid is therefore $\langle\eta_2\rangle = 0$ in the first unit cell and $\langle\eta_2\rangle = 0.5$ in the second one.

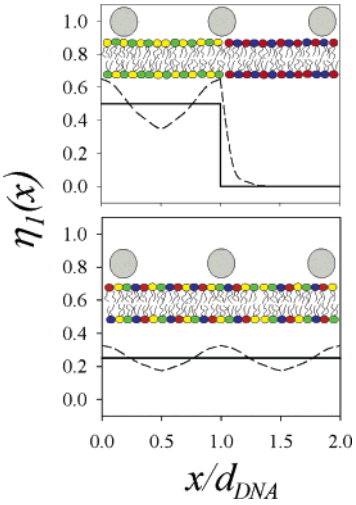

Figure 7. Spatial modulations of the charge of one kind of cationic lipid (DOTAP or DC-Chol) within two adjacent unit cells of multicomponent L_α^C lipoplexes. The local charge profile, $\eta_1(x)$, is affected by lipid mixing. In the top panel, unmixed binary lipoplexes coexist. As a result, $\eta_1(x) = 0.5$ within a unit cell and is equal to zero in the second one. In the case of ideally mixed lipoplexes (bottom panel) the local charge density profile is uniform and equals $\eta_1(x) = 0.25$.

When only mixed lipoplexes exist, the average fraction of both charged lipids is constant all over the spatial extension of two adjacent unit cells and equals $\langle\eta_1\rangle = \langle\eta_2\rangle = 0.25$.

In the case of quaternary lipoplexes, the 2D lipid mixing entropy of eq 5 comes to be

$$F^{\mathrm{MIX}} = \frac{k_\mathrm{B}T}{a}\int_{2S}\left[\sum_{i=1}^{2}\eta_i\ln\eta_i + (1-\eta_i)\ln(1-\eta_i)\right]\mathrm{d}S \quad (6)$$

where η_i is the molar fraction of the ith cationic lipid species.

The integral extends over the membrane area of two adjacent unit cells, $2S$. By geometric arguments, it is easy to recognize that $2S = 2d_{\mathrm{DNA}}\xi$, where ξ is an arbitrary length along the z axis, and it is usually assumed to be the persistence length of DNA, $\xi \approx 500$ Å.

In the case of unmixed lipoplexes (Figure 7, top panel), performing the integral leads to the following expression of 2D lipid mixing entropy, expressed in ($k_\mathrm{B}T$) units,

$$F_\mathrm{I}^{\mathrm{MIX}} = \frac{1}{a}\int_{2S}\left[\sum_{i=1}^{2}\eta_i\ln\eta_i + (1-\eta_i)\ln(1-\eta_i)\right]\mathrm{d}S = \int_S[\eta_1\ln\eta_1 + (1-\eta_1)\ln(1-\eta_1)]\,\mathrm{d}S + \int_S[\eta_2\ln\eta_2 + (1-\eta_2)\ln(1-\eta_2)]\,\mathrm{d}S = -\frac{2\xi d_{\mathrm{DNA}}}{a}\ln 2 \quad (7)$$

Likewise, in the fully mixed state, the 2D lipid mixing entropy (in $k_\mathrm{B}T$ units) reads

$$F_\mathrm{II}^{\mathrm{MIX}} = \frac{1}{a}\int_{2S}\left[\sum_{i=1}^{2}\eta_i\ln\eta_i + (1-\eta_i)\ln(1-\eta_i)\right]\mathrm{d}S = -\frac{2\xi d_{\mathrm{DNA}}}{a}\ln 4 \quad (8)$$

We define $\tilde{F}^{MIX} = F^{MIX}/2\xi d_{DNA}$ as the free energy (in k_BT units) per unit area. Subtracting $\tilde{F}_I^{MIX}$ from $\tilde{F}_{II}^{MIX}$ one can obtain a decrease in free energy, $\Delta\tilde{F}^{MIX} = \tilde{F}_{II}^{MIX} - \tilde{F}_I^{MIX} = -\ln(2)/a$.

Thus, a decrease in free energy due to lipid mixing can successfully explain the existence of only mixed lipoplexes, as revealed by synchrotron SAXD experiments. We claim that 2D lipid mixing entropy is therefore the driving force regulating the spontaneous formation of multicomponent lipoplexes. As shown by Harries et al.,[14] the lateral distribution of cationic lipids in the unit cell of the complex is not exactly uniform. To effectively screen the negative DNA charges, cationic lipids could be pushed out from between the DNA positions. Even though a slight charge modulation could in principle occur (Figure 7, dashed lines) here we refer to uniform local density.

V. Conclusion

In summary, we have looked at the simultaneous interaction of different populations of liposomes with DNA. These experiments gave us a unique overview on the formation process and allowed us to recognize that, during lipoplex formation, large lipid mixing occurs. Such a lipid mixing was found to be the driving force for the entropy driven formation of only mixed lipoplexes by reducing the free energy of the unit cell of the complex. The equilibrium structure of mixed lipoplexes is unique and does not depend on the method of preparation, i.e., on the kind and number of populations of liposomes, but only on the lipid species involved and on their relative molar ratio. Our experimental findings have also highlighted the possibility of rationally designing the structural and physical properties of lamellar lipoplexes by simply adjusting their lipid composition. On the basis of the reported results, multicomponent lipoplexes may represent an important and promising alternative to current binary lipoplexes.

Acknowledgment. The authors thank the reviewers for the many suggestions useful to improving this work.

References and Notes

(1) Salditt, T.; Koltover, I.; Rädler, J. O.; Safinya, C. R. *Phys. Rev. Lett.* **1997**, *79*, 2582.
(2) Koltover, I.; Salditt, T.; Rädler, J. O.; Safinya, C. R. *Science* **1998**, *281*, 78.
(3) Artzner, F.; Zantl, R.; Rapp, G.; Rädler, J. O. *Phys. Rev. Lett.* **1998**, *81*, 5015.
(4) Salditt, T.; Koltover, I.; Rädler, J. O.; Safinya, C. R. *Phys. Rev. E* **1998**, *58*, 889.
(5) Koltover, I.; Salditt, T.; Safinya, C. R. *Biophys. J.* **1999**, *77*, 915.
(6) Caracciolo, G.; Caminiti, R.; Natali, F.; Congiu Castellano, A. *Chem. Phys. Lett.* **2002**, *366*, 200.
(7) Lin, A. J.; Slack, N. L.; Ahmad, A.; Koltover, I.; George, C. X.; Samuel, C. E.; Safinya, C. R. *J. Drug Target.* **2000**, *8*, 13.
(8) Caracciolo, G.; Pozzi, D.; Caminiti, R.; Congiu Castellano,A. *Eur. Phys. J. E* **2003**, *10*, 331.
(9) Huebner, S.; Battersby, B. J.; Grimm, R.; Cevc, G. *Biophys. J.* **1999**, *76*, 3158.
(10) Kinnunen, P. K. J.; Holopainen, J. M. *Biosci. Rep.* **2000**, *6*, 465.
(11) Hayes, M. E.; Gorelov, A. V.; Dawson, K. A. *Prog. Colloid Polym. Sci.* **2001**, *118*, 243.
(12) Barreleiro, P. C. A.; May, R. P.; Lindman, B. *Faraday Discuss.* **2002**, *122*, 191.
(13) Barreleiro, P. C. A.; Lindman, B. *J. Phys. Chem. B* **2003**, *107*, 6208.
(14) Harries, D.; May, S.; Gelbart, W. M.; Ben-Shaul, A. *Biophys. J.* **1998**, *75*, 159.
(15) Caracciolo, G.; Pozzi, D.; Amenitsch, H.; Caminiti, R. *Langmuir* **2005**, *21*, 11582.
(16) Caracciolo, G.; Pozzi, D.; Caminiti,R.; Amenitsch, H. *Appl. Phys. Lett.* **2005**, *87*, 133901.
(17) Caracciolo, G.; Sadun, C.; Caminiti, R.; Pisani, M.; Bruni, P.; Francescangeli, O. *Chem. Phys. Lett.* **2004**, *397*, 138.
(18) Amenitsch, H.; Rappolt, M.; Kriechbaum, M.; Mio, H.; Laggner, P.; Bernstorff, S. *J. Synchrotron Radiat.* **1998**, *5*, 506.
(19) Luzzati, V.; Mariani, P.; Delacroix, H. *Makromol. Chem., Macromol. Symp.* **1988**, *15*, 1.
(20) Luzzati, V. In *Biological Membranes*; Academic Press: New York, 1968.
(21) Pabst, G.; Rappolt, M.; Amenitsch, H.; Laggner, P. *Phys. Rev. E* **2000**, *62*, 4000.
(22) Hauser, H. *Biochim. Biophys. Acta* **1984**, *772*, 37.
(23) Israelachvili, J. *Intermolecular and Surface Forces*; Academic Press: London, UK, 1991.
(24) Oberle, V.; Bakowsky, U.; Zuhorn, I. S.; Hoekstra, D. *Biophys. J.* **2000**, *79*, 1447.
(25) Tarahovsky, Y. S.; Koynova, R.; MacDonald, R. C. *Biophys. J.* **2004**, *87*, 1054.
(26) Koltover, I.; Wagner, K.; Safinya, C. R. *Proc. Natl. Acad. Sci. U.S.A.* **2000**, *97*, 14046.
(27) Safinya, C. R. *Curr. Opin. Struct. Biol.* **2001**, *11*, 440.
(28) Caracciolo, G.; Caminiti, R.; Pozzi, D.; Friello, M.; Boffi, F.; Congiu Castellano A. *Chem. Phys. Lett.* **2002**, *351*, 222.
(29) Caracciolo, G.; Caminiti, R. *Chem. Phys. Lett.* **2004**, *400*, 314.
(30) Kennedy, M. T.; Pozharski, E. V.; Rakhmanova, V. A.; MacDonald, R. C. *Biophys. J.* **2000**, *78*, 1620.
(31) May, S.; Ben-Shaul, A. *Curr. Med. Chem.* **2004**, *11*, 1241.
(32) May, S. *J. Phys.: Condens. Matter* **2005**, *17*, 833.